



## Thermoelectric properties of boron carbide/HfB<sub>2</sub> composites

Jon-L Innocent, David Portehault, Guillaume Gouget, Satofumi Maruyama, Isao Ohkubo, Takao Mori

### ► To cite this version:

Jon-L Innocent, David Portehault, Guillaume Gouget, Satofumi Maruyama, Isao Ohkubo, et al.. Thermoelectric properties of boron carbide/HfB<sub>2</sub> composites. Materials for Renewable and Sustainable Energy, 2017, 6 (2), pp.6. 10.1007/s40243-017-0090-8 . hal-01517701

HAL Id: hal-01517701

<https://hal.sorbonne-universite.fr/hal-01517701>

Submitted on 3 May 2017

**HAL** is a multi-disciplinary open access archive for the deposit and dissemination of scientific research documents, whether they are published or not. The documents may come from teaching and research institutions in France or abroad, or from public or private research centers.

L'archive ouverte pluridisciplinaire **HAL**, est destinée au dépôt et à la diffusion de documents scientifiques de niveau recherche, publiés ou non, émanant des établissements d'enseignement et de recherche français ou étrangers, des laboratoires publics ou privés.



Distributed under a Creative Commons Attribution 4.0 International License

# Thermoelectric properties of boron carbide/HfB<sub>2</sub> composites

Jon-L. Innocent<sup>1,4</sup> · David Portehault<sup>2</sup> · Guillaume Gouget<sup>2,5</sup> · Satofumi Maruyama<sup>1,6</sup> · Isao Ohkubo<sup>1</sup> · Takao Mori<sup>1,3</sup>

Received: 27 September 2016 / Accepted: 21 March 2017  
© The Author(s) 2017. This article is an open access publication

**Abstract** Boron carbide/hafnium diboride composites were prepared by spark plasma sintering of a mixture of hafnium diboride and boron carbide powders. Boron carbide was prepared with a 13.3 at.% composition of carbon, known as the ideal carbon content to maximize the dimensionless figure of merit. The hafnium diboride content was varied between 0 and 20% by weight, and the effect on the thermoelectric properties was studied. Addition of HfB<sub>2</sub> generally yielded an increase in the electrical conductivity and simultaneously a reduction in thermal conductivity, indicating it has potential as an enhancer of thermoelectric properties. However, the increase in electrical conductivity was not as large as observed in some composite systems, since HfB<sub>2</sub> turned out to be a poor sintering additive leading to lower relative densities, and was furthermore offset by a moderate decrease in Seebeck coefficient. For future composite design, the sintering

characteristics of the additives can be concluded as an important additional parameter to be taken into account. The optimal hafnium diboride content for relatively dense samples was found to be 10 wt%, resulting in an improvement in the maximum figure of merit, up to  $ZT = 0.20$  at 730 °C.

**Keywords** Thermoelectric · Boride · Composite · Spark plasma sintering

## Introduction

Thermoelectric energy generation is an increasingly intriguing prospect for use in producing green energy, particularly from waste heat processes [1]. Recent discoveries of several new classes of thermoelectric materials like cage-structured PGECs (phonon glass electron crystal systems) [2–5], nanostructured materials [6–10] and magnetic semiconductors [11–13] have incited a renewed interest in thermoelectric materials development. The performance of thermoelectric materials can be gauged by the figure of merit  $ZT = S^2T/\rho\kappa$ , where  $S$ ,  $\rho$ ,  $\kappa$  and  $T$  are the Seebeck coefficient, electrical resistivity, thermal conductivity and absolute temperature, respectively. A need exists for high-temperature thermoelectric materials which can be used to convert waste heat from thermal power plants, steelworks, factories, incinerators, etc. [14–16]. Boron cluster compounds are attractive candidates for this need because of their high stability and relatively high Seebeck coefficients [17–19]. They also exhibit relatively low thermal conductivity [20–22]. Several mechanisms have been proposed to explain the low thermal conductivity [23, 24]. Namely, large number of atoms in the unit cell (i.e., crystal complexity) disorder due to typical partial

✉ Takao Mori  
MORI.Takao@nims.go.jp

<sup>1</sup> MANA, National Institute for Materials Science (NIMS), Namiki 1-1, Tsukuba 305-0044, Japan

<sup>2</sup> Sorbonne Universités-UPMC Univ. Paris 06, CNRS, Collège de France, Laboratoire de Chimie de la Matière Condensée de Paris, 4 place Jussieu, 75252 Paris Cedex 05, France

<sup>3</sup> Graduate School of Pure and Applied Sciences, University of Tsukuba, 1-1-1 Tennoudai, Tsukuba 305-8671, Japan

<sup>4</sup> Present Address: Colombia University, 116th and Broadway, New York, NY 10027, USA

<sup>5</sup> Present Address: Institut de Chimie de la Matière Condensée de Bordeaux, CNRS, 87 avenue du Dr. A. Schweitzer, 33600 Pessac, France

<sup>6</sup> Present Address: Tokyo City University (TCU), Setagaya, Tokyo 158-8557, Japan

occupancies of atomic sites in these crystal structures, possible rattling of metal atoms in the voids among the boron cluster structure. An interesting possibility raised is the symmetry mismatch effect, where the prominent symmetry of a basic building block of the structure, the  $B_{12}$  icosahedron, has a mismatch with the symmetry of the structure. However, clear proof of this effect has not yet been presented [24]. Regarding the electrical properties, boron cluster compounds in general show the variable range hopping (VRH) behavior where both the Seebeck coefficient and electrical conductivity increase with increasing temperature [18, 25]. These features are inherently desirable for thermoelectric energy generation, and particularly so for high-temperature applications. Well-known boron compounds like boron carbide [17, 26–28] have been investigated for thermoelectrics, with recent striking p, n control demonstrated in Zr-doped  $\beta$ -boron [29],  $YAl_xB_{14}$  [30–32] and later also  $MgAlB_{14}$  [33, 34]. A renewed interest in  $RB_{66}$  [22, 35] has also arisen with large enhancements in  $ZT$  discovered for  $YB_{48}$  [36] and  $SmB_{66}$  [37]. The n-type counterparts to boron carbide; the rare earth borocarbonitrides [38–41] are also of interest. Regarding research for application of thermoelectric borides, it is striking that manufacture and testing of thermoelectric bulk modules containing boron carbide at elevated temperatures have been carried out recently [42].

Previous research has shown that the performance of boron carbide is affected by the carbon content of the material [14, 24]. It has been found that the ideal carbon content for the thermoelectric figure of merit  $ZT$  is 13.3 at.% carbon [24]. It has also been shown that the addition of some metal-borides to form a composite material can improve the figure of merit [43–46]. For example,  $TiB_2$  doped into boron carbide [43, 44] and  $CoB$  and  $VB_2$  doped into  $YB_{22}C_2N$  [45, 46]. A recent review on the thermoelectric enhancement in composites has also been given [47]. In this work, the effect of hafnium diboride doping on the thermoelectric properties of boron carbide was studied.

## Experimental

Spark plasma sintering (SPS) was used to prepare samples of boron carbide/hafnium diboride composite material. Polycrystalline samples of boron carbide, in the composition of  $B_{13}C_2$ , were first synthesized by the conventional solid-state reaction process. Amorphous boron (SB Boron 99.9%) and carbon (Wako 99.9%) powders were mixed, pressed using cold isostatic press (CIP) and heated up to around 1800 °C for 12 h in vacuum using an induction furnace. The resulting polycrystalline boron carbide powder was combined with  $HfB_2$  powder (Hermann Starck Co.

99.9%) in 0–20 wt% ratios. The composite powder was prepared by grinding the materials using a pestle and mortar in ethanol to promote homogeneity of the samples. The dried powder was then placed into a graphite dye and pressed for sintering. The SPS was performed in vacuum at 1750 °C for 6 min after a 10-min ramp-up process, for 10-mm-diameter samples under 50 MPa pressure.

The samples were characterized using high-resolution powder X-ray diffraction (XRD). Powder XRD measurements with  $CuK_\alpha$  radiations (Rigaku Ultima-3) were taken to confirm the sample composition.

Resistivity and Seebeck coefficient were measured simultaneously with an ULVAC ZEM-2 in the temperature range of 323–1005 K in  $N_2$  atmosphere. Specific heat and thermal diffusivity coefficients were measured by the laser flash method (ULVAC TC-7000) from 300 to 1003 K. Thermal conductivity was determined as the product of the density, specific heat and thermal diffusivity coefficient.

## Results and discussion

### XRD measurements

XRD patterns (Fig. 1) exhibit for all the samples only main peaks corresponding to boron carbide and hafnium diboride, indicating successful synthesis of the composites. There are some small minor peaks at  $2\theta = 27^\circ$  and  $2\theta = 13.4^\circ, 33.6^\circ, 36^\circ$ , which correspond to peaks of C graphite assumedly from the SPS dye and  $BC_5$  [48], respectively. The smallness of these peaks indicates that any effect on the physical properties is not likely to be large.

XRD measurements show that the relative heights of the peaks which correspond to hafnium diboride increase with the increasing hafnium diboride composition, as expected.

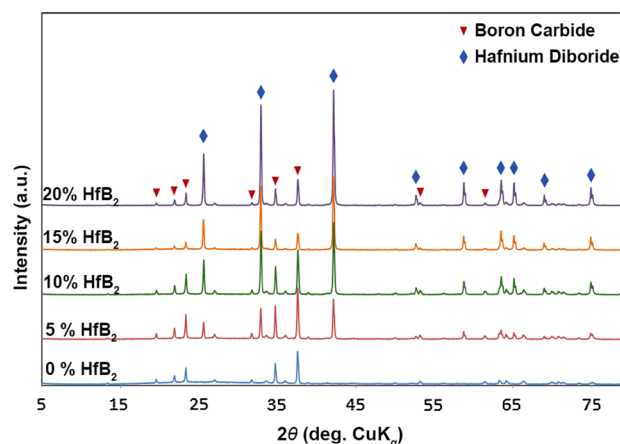


**Fig. 1** X-ray diffraction data for composite samples showing relative peak heights

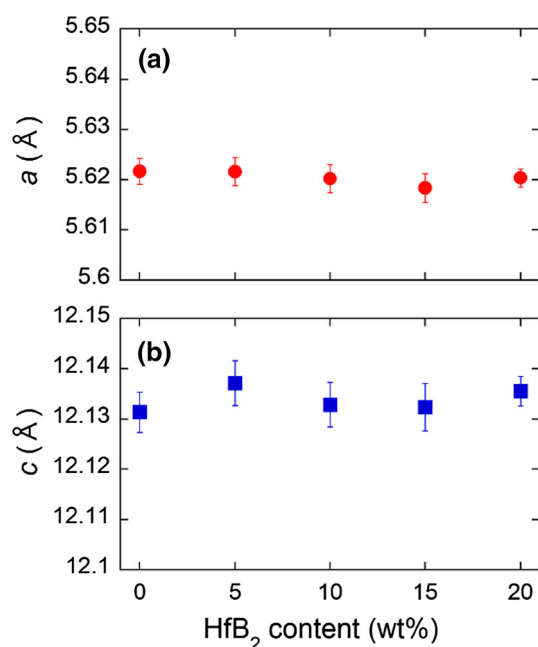


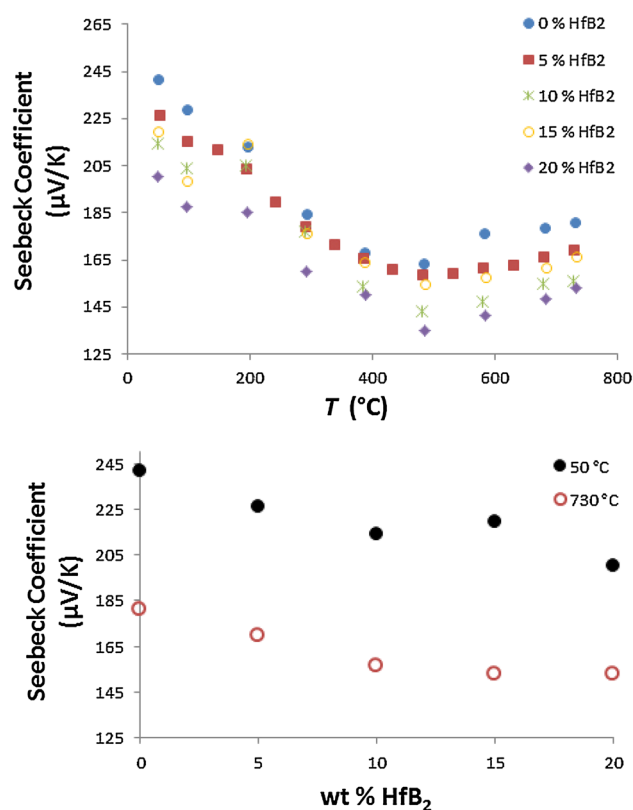
**Fig. 2** Effect of the HfB<sub>2</sub> content on the lattice parameters of boron carbide

The absence of peak position shift suggests that the crystal structure is not affected by the addition of HfB<sub>2</sub>, as expected for a composite sample. To confirm this conclusion, the lattice constant of the boron carbide matrix was evaluated by Rietveld refinement as a function of the HfB<sub>2</sub> composition (Fig. 2). As lattice constants of boron carbide with different HfB<sub>2</sub> compositions were almost unchanged, all the composite samples appeared to have the same crystal structure of boron carbide. This also indicates that the addition of HfB<sub>2</sub> did not affect the boron carbide phase in the composite samples.

### Thermoelectric measurements

The thermoelectric properties were measured for each sample with varying hafnium diboride composition across a temperature range, in order to determine how thermoelectric properties depend on both composition and temperature.

For all compositions, the Seebeck coefficient first decreases with temperature, then increases with temperature beyond approximately 480 °C (Fig. 3). The temperature dependence is different from the monotonic increase in pure boron carbide and therefore is a composite effect from metallic hafnium diboride. Noteworthy, the increasing Seebeck coefficient at high temperatures above 480 °C makes it a favorable material for high-temperature applications.



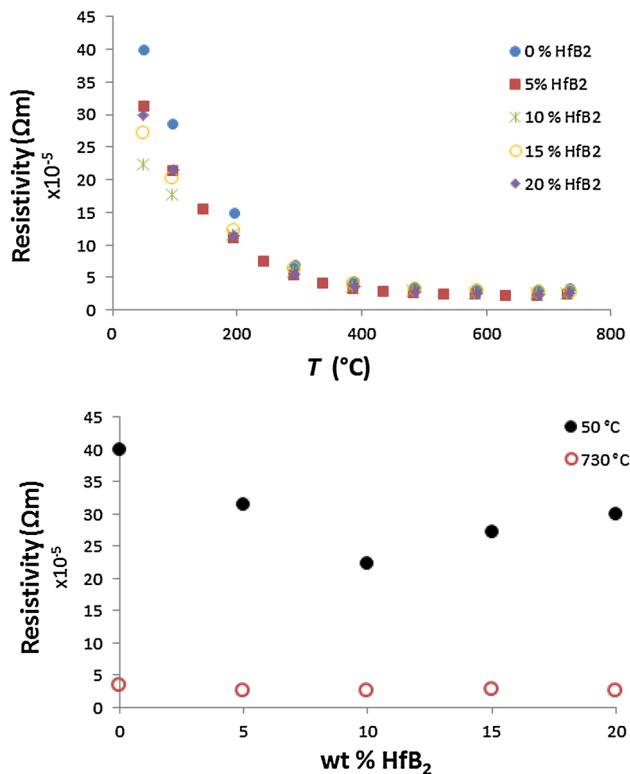
**Fig. 3** Seebeck coefficient as a function of (top) temperature and (bottom) hafnium diboride composition

Figure 3 shows that the Seebeck coefficient decreases with increasing HfB<sub>2</sub> composition. This is expected because boron carbide is being replaced by metallic HfB<sub>2</sub> with a small Seebeck coefficient. Therefore, the overall composite material should have a lower Seebeck coefficient.

Similarly, the electrical resistivity of the samples was compared with changing temperature and composition (Fig. 4). The electrical resistivity decreases with temperature for all the compositions examined. The electrical resistivity shows a more complex behavior: Below 400 °C, it decreases with increasing HfB<sub>2</sub> content up to 10 wt%, then increases. At higher temperature, the resistivity at first glance does not appear to depend on the HfB<sub>2</sub> content.

This result is unusual because the resistivity would be expected to continuously decrease with increasing HfB<sub>2</sub> composition. To understand this surprising behavior, the sample absolute and relative densities were measured (Fig. 5) for all the boron carbide/hafnium diboride composites.

As the HfB<sub>2</sub> content is increased, it can be observed that the relative densities monotonically significantly decrease. This indicates that hafnium diboride hinders the sintering



**Fig. 4** Electrical resistivity as a function of (top) temperature and (bottom) hafnium diboride composition

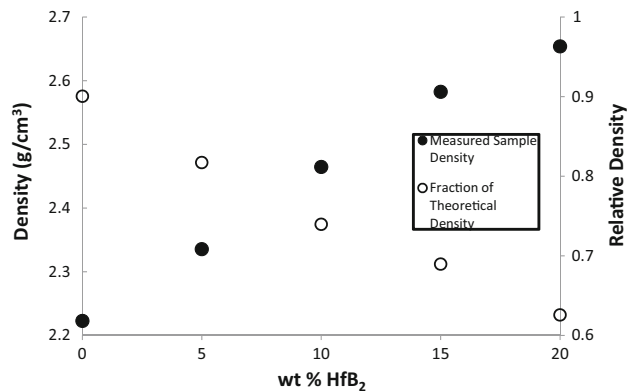


**Fig. 5** Boron carbide/hafnium diboride composite samples; densities and fraction of theoretical densities, i.e., relative densities

of boron carbide. This decrease in relative density accounts for the relatively small increase in electrical conductivity with metallic additives compared to other previously composites [39, 45, 46]. Poor sintering also accounts for the peculiar composition dependence of electrical resistivity (Fig. 4). For future composite design, we can conclude that the sintering characteristics of the additives are an important additional parameter to be taken into account. Recently, data-mining/material informatics approaches have been used to search for viable thermoelectric materials [49]. It would accelerate research if such sintering

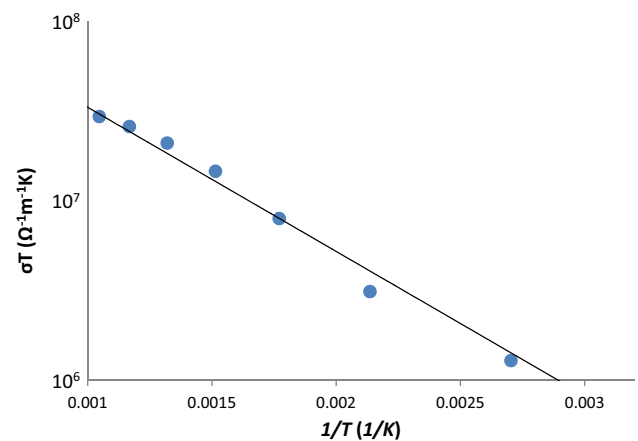


**Fig. 6** Plot of  $\ln(\sigma T)$  versus reciprocal temperature for undoped boron carbide

characteristics could also be incorporated as a parameter in the search for effective additives to enhance overall thermoelectric performance.

The electrical resistivity data were fitted to a polaron hopping model suggested by Wood et al. [17]. According to the model, the hopping motion of a temperature-independent density of small-polaron holes leads to a temperature dependence of conductivity which corresponds to that of the mobility ( $\mu$ ). Above approximately 1/3 of the characteristic phonon temperature, this small-polaron hopping gives rise to a thermally activated mobility which has a prefactor that is temperature dependent. The charge follows the atomic motion adiabatically which results in a temperature dependence of the mobility given by

$$\mu \propto T^{-1} \exp\left(\frac{-E_A}{kT}\right) \quad (1)$$

where  $E_A$  represents the mobility activation energy. In order to evaluate the fit of our data to this model, the logarithm of the product of the electrical conductivity  $\sigma$  and the absolute temperature was plotted against the inverse of the absolute temperature (Figs. 6, 7).

The hafnium diboride-doped samples show a more pronounced curvature than the undoped sample when compared to the straight line fit (Fig. 7). Figures 6 and 7 indicate that the addition of hafnium diboride alters the electrical conductivity dependence on the temperature such that it no longer is well described by the polaron hopping model suggested by Wood et al. [17]. This is expected as the governing mechanism for charge carrier transport in a composite sample is more complex than that of a single material, and furthermore, the effect of the lower relative densities on the temperature dependence is not trivial. Regarding the apparent convergence of the resistivity data of all samples above 400  $^{\circ}\text{C}$  in Fig. 4, the plot above in Fig. 7 shows the differences. However, at higher

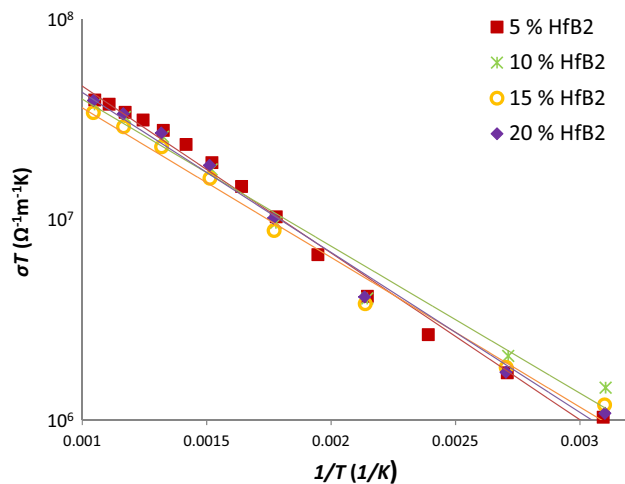


**Fig. 7** Plot of  $\ln(\sigma T)$  versus reciprocal temperature of boron carbide/HfB<sub>2</sub> composites for various sample compositions

temperatures, although the 15% sample is an outlier, there is a convergence tendency compared to the points below 400 °C, and this can be considered to be because the intrinsic hopping in the boron carbide material relatively becomes more active compared to the composite effect of the added metallic component and also the porosity effect of the different densities.

The thermal conductivity was found to decrease with increasing HfB<sub>2</sub> composition. At 100 °C, the thermal conductivity was found to be 4.56, 4.52 and 4.28 W/mK for the 0, 5 and 10% samples, respectively. We utilize the Eucken model [50, 51] as a rough estimation to try to gauge the effects of porosity on the effective thermal conductivity  $\kappa_{\text{eff}}$ :

$$\kappa_{\text{eff}} \approx \kappa_m [2(1 - \phi)/(2 + \phi)], \quad (2)$$

where  $\phi$  is the porosity and  $\kappa_m$  is the bulk thermal conductivity. We use the experimentally determined values of porosity (Fig. 5) and normalizing at the value for the 0% doped sample would yield 3.98 and 3.48 W/mK for the 5 and 10% samples, respectively. Therefore, it is indicated that intrinsically the HfB<sub>2</sub> dopant is not functioning as an effective phonon scatterer, despite the heavy mass of hafnium. We cannot simply estimate the effect of porosity on the electrical conductivity. However, previous results in borides indicate that the penalty from reduction in electrical conductivity with porosity typically largely outweighs the benefit in reduction in thermal conductivity [30, 32, 39]. As a result, there have been many efforts to densify thermoelectric borides [30, 32, 39, 40, 52]. Therefore, the fact that in relatively dense samples, the doping of HfB<sub>2</sub> results in an overall reduction in the thermal conductivity, in contrast to the increase in electrical conductivity, indicates the potential of HfB<sub>2</sub> as an enhancer of thermoelectric properties. In combination with

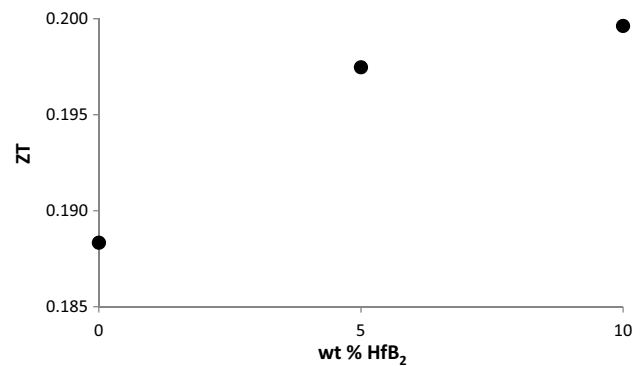


**Fig. 8** Figure of merit  $ZT$  versus hafnium diboride composition at 750 °C

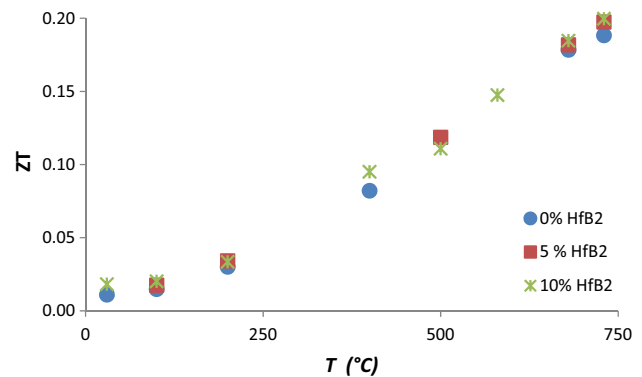


**Fig. 9** Figure of merit  $ZT$  versus temperature of boron carbide/HfB<sub>2</sub> composites for 0–10 wt% hafnium diboride samples

boron carbide, we can surmise that it would be effective to search for a similar metallic boride albeit with better sintering effects to use in a composite.

The thermoelectric figure of merit  $ZT$  (Fig. 8) was calculated for HfB<sub>2</sub> contents below 10 wt%, where the relative density is still sufficiently high.  $ZT$  appears to be maximized for the 10 wt% HfB<sub>2</sub> sample. The  $ZT$  value for each sample still increases with temperature within the temperature range investigated (Fig. 9).

The  $ZT$  value was increased from 0.19 for the non-composite material to 0.20 for the 10% wt HfB<sub>2</sub> composite at 730 °C, corresponding to an increase of 5%. This increase with HfB<sub>2</sub> incorporation is modest. This small effect is likely originating from the relatively small increase in the electrical conductivity due to the lower relative densities. This effect is also coupled with the reduction in the Seebeck coefficient for the composite samples. It has previously been observed for VB<sub>2</sub>-seeded YB<sub>22</sub>C<sub>2</sub>N that Seebeck coefficients can increase when partial intrinsic doping assumedly occurred from heat treatment [45–47]. This effect may also impact the figure of merit of the composite and should be investigated in the future. Looking for metallic borides with better



sintering properties than  $\text{HfB}_2$  as an additive to boron carbide is also worthwhile.

## Conclusions and future work

The addition of hafnium diboride to boron carbide to form a composite material showed an improvement in the overall thermoelectric performance of boron carbide, in spite of the poor sintering characteristics of the additive. The measurements show that the decrease in the value of the Seebeck coefficient caused by the addition of  $\text{HfB}_2$  can be countered by the relatively larger decrease in both thermal conductivity and electrical resistivity. This is obtained despite the monotonic reduction in the relative densities of the samples with  $\text{HfB}_2$  addition which is very detrimental to electrical conductivity. A maximum  $ZT = 0.20$  at  $730^\circ\text{C}$  is obtained for  $\text{HfB}_2$  content of 10 wt%. One can expect higher  $ZT$  values for better densified composites.

For future composite design, we can conclude that the sintering characteristics of the additives are an important parameter to be taken into account. It is worth further investigating similar metallic borides albeit with better sintering effect to use in a composite. Recently, data-mining/material informatics approaches have gathered increasing interest in materials development. Herein we highlight the fact that besides intrinsic properties of each constituents, computational materials design could provide a more effective impetus to the field of thermoelectricity if computations could also take into account sintering characteristics. This would eventually optimize the search for effective additives to enhance overall thermoelectric performance.

In general, boron carbide-based materials have excellent potential as high-temperature thermoelectric materials since both the Seebeck coefficient and electrical conductivity increase with temperature while the thermal conductivity is relatively small with little temperature dependence at high temperatures [42, 53], leading to a  $ZT$  value which increases strongly with temperature. We are also planning further experiments with suitable instrumentation to measure the thermoelectric properties at higher temperatures (with better densified materials) as the  $ZT$  value is expected to still increase beyond the temperature range investigated in the present study.

**Acknowledgements** J.L.I. was supported by the NNIN internship program. Support is acknowledged from “Materials Research by Information Integration” Initiative (MI2I) and JSPS KAKENHI Grant Number JP16H064xx. This work was conceived by T.M., D.P. and G.G. J.L.I. carried out the main experimental work. S.M. assisted J.L.I. with the use of synthesis and measurement apparatuses and Rietveld, and I. O. gave research advice. J.L.I. mainly wrote the initial

draft of the paper with revisions being written and carried out by T.M., D.P. and G.G.

**Open Access** This article is distributed under the terms of the Creative Commons Attribution 4.0 International License (<http://creativecommons.org/licenses/by/4.0/>), which permits unrestricted use, distribution, and reproduction in any medium, provided you give appropriate credit to the original author(s) and the source, provide a link to the Creative Commons license, and indicate if changes were made.

## References

1. Koumoto, K., Mori, T. (eds.): Thermoelectric Nanomaterials—Materials Design and Applications, vol. 182. Springer Series in Materials Science. Springer, Heidelberg (2013)
2. Slack, G.A., Tsoukala, V.G.: Some properties of semiconducting  $\text{IrSb}_3$ . *J. Appl. Phys.* **76**, 1635 (1994)
3. Uher, C.: In: Tritt, T.M. (ed.) Semiconductors and Semimetals, vol. 69, p. 139. Academic Press, New York (2000)
4. Nolas, G.S., Morelli, D.T., Tritt, T.M.: SKUTTERUDITES: a Phonon-Glass-Electron Crystal Approach to Advanced Thermoelectric Energy Conversion Applications. *Annu. Rev. Mater. Sci.* **29**, 89 (1999)
5. Saiga, Y., Du, B., Deng, S.K., Kajisa, K., Takabatake, T.: Thermoelectric properties of type-VIII clathrate  $\text{Ba}_8\text{Ga}_{16}\text{Sn}_{30}$  doped with Cu. *J. Alloys Compd.* **537**, 303–307 (2012)
6. Zhao, X.B., Ji, X.H., Zhang, Y.H., Zhu, T.J., Tu, J.P., Zhang, X.B.: Bismuth telluride nanotubes and the effects on the thermoelectric properties of nanotube-containing nanocomposites. *Appl. Phys. Lett.* **86**, 06211 (2005)
7. Poudel, B., Hao, Q., Ma, Y., Lan, Y.C., Minnich, A., Yu, B., Yan, X., Wang, D.Z., Muto, A., Vashaee, D., Chen, X.Y., Liu, J.M., Dresselhaus, M.S., Chen, G., Ren, Z.F.: High-thermoelectric performance of nanostructured bismuth antimony telluride bulk alloys. *Science* **320**, 634–638 (2008)
8. Biswas, K., He, J.Q., Blum, I.D., Wu, C.I., Hogan, T.P., Seidman, D.N., Droid, V.P., Kanatzidis, M.G.: High-performance bulk thermoelectrics with all-scale hierarchical architectures. *Nature* **489**, 414–418 (2012)
9. Rogl, G., Setman, D., Schaffler, E., Horky, J., Kerber, M., Zehetbauer, M., Falmbigl, M., Rogl, P., Royanian, E., Bauer, E.: High-pressure torsion, a new processing route for thermoelectrics of high  $ZT$ s by means of severe plastic deformation. *Acta Mater.* **60**(5), 2146 (2012)
10. Khan, A.U., Kobayashi, K., Tang, D., Yamauchi, Y., Hasegawa, K., Mitome, M., Xue, Y., Jiang, B., Tsuchiya, K., Golberg, D., Bando, Y., Mori, T.: Nano-micro-porous skutterudites with 100% enhancement in  $ZT$  for high performance thermoelectricity. *Nano Energy* **31**, 152 (2017)
11. Tsujii, N., Mori, T.: High thermoelectric power factor in a carrier-doped magnetic semiconductor  $\text{CuFeS}_2$ . *Appl. Phys. Express* **6**, 043001 (2013)
12. Ang, R., Khan, A.U., Tsujii, N., Takai, K., Nakamura, R., Mori, T.: Thermoelectricity generation and electron–magnon scattering in a natural chalcopyrite mineral from a deep-sea hydrothermal vent. *Angew. Chem. Int. Ed.* **54**, 12909 (2015)
13. Lefèvre, R., Berthebaud, D., Mychinko, M.Yu., Lebedev, O.I., Mori, T., Gascoin, F., Maignan, A.: Thermoelectric properties of the chalcopyrite  $\text{Cu}_{1-x}\text{M}_x\text{FeS}_{2-y}$  series ( $\text{M} = \text{Mn}, \text{Co}, \text{Ni}$ ). *RSC Adv.* **6**, 55117–55124 (2016)
14. Mori, T.: Perspectives of high-temperature thermoelectric applications and p-type and n-type aluminoborides. *JOM* **68**, 2673–2679 (2016)

15. Terasaki, I., Okazaki, R., Mondal, P.S., Hsieh, Y.C.: Trials for oxide photo-thermoelectrics. *Mater. Renew. Sustain. Energy* **3**, 29 (2014)
16. Day, T.W., Borup, K.A., Zhang, T., Drymiotis, F., Brown, D.R., Shi, X., Chen, L., Iversen, B.B., Snyder, G.J.: High-temperature thermoelectric properties of  $\text{Cu}_{1.97}\text{Ag}_{0.03}\text{Se}_{1+y}$ . *Mater. Renew. Sustain. Energy* **3**, 26 (2014)
17. Wood, C., Emin, D.: Conduction mechanism in boron carbide. *Phys. Rev. B* **29**, 4582 (1984)
18. Mori, T., Berthebaud, D., Nishimura, T., Nomura, A., Shishido, T., Nakajima, K.: Effect of Zn doping on improving crystal quality and thermoelectric properties of borosilicides. *Dalton Trans.* **2010**, 39 (1027)
19. Mori, T.: Higher borides. In: Gschneidner Jr., K.A., Bunzli, J.-C., Pecharsky, V.K. (eds.) *Handbook on the Physics and Chemistry of Rare Earths*, vol. 38, pp. 105–173. Elsevier, Amsterdam (2008)
20. Slack, G.A., Oliver, D.W., Horn, F.H.: Thermal conductivity of boron and some boron compounds. *Phys. Rev. B* **4**, 1714 (1971)
21. Cahill, D.G., Fischer, H.E., Watson, S.K., Pohl, R.O., Slack, G.A.: Thermal properties of boron and boride. *Phys. Rev. B* **40**, 3254 (1989)
22. Mori, T.: Thermal conductivity of a rare-earth  $\text{B}_{12}$ -icosahedral compound. *Phys. B Condens. Matter* **383**, 120 (2006)
23. Mori, T., Martin, J., Nolas, G.: Thermal conductivity of  $\text{YbB}_{44}\text{Si}_2$ . *J. Appl. Phys.* **102**, 073510 (2007)
24. Mori, T.: In: Rowe, D.M. (ed.) *Modules, Systems, and Applications in Thermoelectrics*, p. 14. CRC Press/Taylor and Francis, London (2012)
25. Mori, T., Tanaka, T.: Thermoelectric properties of homologous p- and n-type boron-rich borides. *J. Solid State Chem.* **179**, 2889 (2006)
26. Aselage, T.L., Emin, D., McCready, S.S., Duncan, R.V.: Large enhancement of boron carbides' Seebeck coefficients through vibrational softening. *Phys. Rev. Lett.* **81**, 2316 (1998)
27. Bouchacourt, M., Thevenot, F.: The correlation between the thermoelectric properties and stoichiometry in the boron carbide phase  $\text{B}_4\text{C-B}_{10.5}\text{C}$ . *J. Mater. Sci.* **20**, 1237 (1985)
28. Cai, K.F., Nan, C.W., Min, X.M.: The influence of silicon dopant and processing on thermoelectric properties of  $\text{B}_4\text{C}$  ceramics. In: *Symposium Z—Thermoelectric Materials 1998—The Next Generation*, vol. 545. MRS Online Proceedings Library, Warrendale (1998)
29. Sologub, O., Salamakha, L., Stoger, B., Michiue, Y., Mori, T.: Zr doped  $\beta$ -rhombohedral boron: Widely variable Seebeck coefficient and structural properties. *Acta Mater.* **122**, 378 (2017)
30. Maruyama, S., Nishimura, T., Miyazaki, Y., Hayashi, K., Kajitani, T., Mori, T.: Al insertion and additive effects on the thermoelectric properties of yttrium boride. *J. Appl. Phys.* **115**, 123702 (2014)
31. Sahara, R., Mori, T., Maruyama, S., Miyazaki, Y., Hayashi, K., Kajitani, T.: Theoretical and experimental investigation of the excellent p–n control in yttrium aluminoborides. *Sci. Technol. Adv. Mater.* **15**, 035012 (2014)
32. Maruyama, S., Nishimura, T., Miyazaki, Y., Hayashi, K., Kajitani, T., Mori, T.: Microstructure and thermoelectric properties of  $\text{Y}_x\text{Al}_y\text{B}_{14}$  samples fabricated through the spark plasma sintering. *Mater. Renew. Sustain. Energy* **3**, 31 (2014)
33. Wan, L.F., Beckman, S.P.: Lattice instability in the  $\text{AlMgB}_{14}$  structure. *Phys. B Condens. Matter* **438**, 9 (2014)
34. Miura, S., Sasaki, H., Takagi, K., Fujima, T.: Effect of varying mixture ratio of raw material powders on the thermoelectric properties of  $\text{AlMgB}_{14}$ -based materials prepared by spark plasma sintering. *J. Phys. Chem. Solids* **75**, 951 (2014)
35. Golikova, O.A., Amandzhanov, N., Kazanin, M.M., Klimashin, G.M., Kutasov, V.V.: Electrical activity of impurities in  $\beta$ -rhombohedral boron. *Phys. Status Solidi A* **121**, 579 (1990)
36. Hossain, M.A., Tanaka, I., Tanaka, T., Khan, A.U., Mori, T.:  $\text{YB}_{48}$  the metal rich boundary of  $\text{YB}_{66}$ ; crystal growth and thermoelectric properties. *J. Phys. Chem. Solids* **87**, 221 (2015)
37. Sussardi, A., Tanaka, T., Khan, A.U., Schlapbach, L., Mori, T.: Enhanced thermoelectric properties of samarium boride. *J. Mater. Sci.* **1**, 196 (2015)
38. Mori, T., Nishimura, T.: Thermoelectric properties of homologous p- and n-type boron-rich borides. *J. Solid State Chem.* **179**, 2908 (2006)
39. Mori, T., Nishimura, T., Yamaura, K., Takayama-Muromachi, E.: High temperature thermoelectric properties of a homologous series of n-type boron icosahedra compounds: A possible counterpart to p-type boron carbide. *J. Appl. Phys.* **101**, 093714 (2007)
40. Berthebaud, D., Nishimura, T., Mori, T.: Thermoelectric properties and spark plasma sintering of doped  $\text{YB}_{22}\text{C}_2\text{N}$ . *J. Mater. Res.* **25**, 665 (2010)
41. Mori, T., Nishimura, T., Schnelle, W., Burkhardt, U., Grin, Y.: The origin of the n-type behavior in rare earth borocarbide  $\text{Y}_{1-x}\text{B}_{28.5}\text{C}_4$ . *Dalton Trans.* **43**, 15048 (2014)
42. Feng, B., Martin, H.-P., Börner, F.-D., Lippmann, W., Schreier, M., Vogel, K., Lenk, A., Veremchuk, I., Dannowski, M., Richter, C., Pfeiffer, P., Zikordise, G., Lichte, H., Grin, J., Hurtado, A., Michaelis, A.: Manufacture and Testing of Thermoelectric Modules Consisting of  $\text{B}_x\text{C}$  and  $\text{TiO}_x$  Elements. *Adv. Eng. Mater.* **16**, 1252–1263 (2014)
43. Goto, T.: *Kinzoku* (in Japanese) **68**, 1086 (1998).
44. Bing, F., Martin, H.P., Michaelis, A.: *In Situ* Preparation and Thermoelectric Properties of  $\text{B}_4\text{C}_{1-x}\text{-TiB}_2$  Composites. *J. Electron. Mater.* **42**, 2314–2319 (2013)
45. Prytulak, A., Mori, T.: Effect of Transition-Metal Additives on Thermoelectric Properties of  $\text{YB}_{22}\text{C}_2\text{N}$ . *J. Electron. Mater.* **40**, 920–925 (2011)
46. Prytulak, A., Maruyama, S., Mori, T.: Anomalous effect of vanadium boride seeding on thermoelectric properties of  $\text{YB}_{22}\text{-C}_2\text{N}$ . *Mater. Res. Bull.* **48**, 1972 (2013)
47. Mori, T., Hara, T.: Hybrid effect to possibly overcome the trade-off between Seebeck coefficient and electrical conductivity. *Scr. Mater.* **111**, 44 (2016)
48. Yao, Y., Tse, J.S., Klug, D.D.: Crystal and electronic structure of superhard  $\text{BC}_5$ : First-principles structural optimizations. *Phys. Rev. B* **80**, 094106 (2009)
49. Sparks, T.D., Gaultois, M.W., Oliynyk, A., Brgoch, J., Meredig, B.: Data mining our way to the next generation of thermoelectrics. *Scr. Mater.* **111**, 10 (2016)
50. Eucken, A.: Thermal conductivity of ceramic refractory materials: calculation from thermal conductivities of constituents. *VDI Forschungsheft* **353**, 16 (1932)
51. Eucken, A.: Thermal conductivity of ceramic refractory materials; Its calculation from thermal conductivity of constituents. *Ceram. Abstr.* **12**, 231 (1933)
52. Berthebaud, D., Nishimura, T., Mori, T.: Thermoelectric properties and spark plasma sintering of doped  $\text{YB}_{22}\text{C}_2\text{N}$ . *J. Electron. Mater.* **40**, 682 (2011)
53. Wood, C., Emin, D., Gray, P.E.: Thermal conductivity behavior of boron carbides. *Phys. Rev. B* **31**, 6811 (1985)